

Volume Flows and Pressure Changes During an Action Potential in Cells of *Chara australis*

II. Theoretical Considerations

PETER H. BARRY*

Biophysics Laboratory, School of Biological Sciences, Flinders University,
Bedford Park, South Australia 5042, and Department of Physiology,
School of Medicine, Center for the Health Sciences, University of California,
Los Angeles, California 90024

Received 20 May 1970

Summary. It has been suggested that electro-kinetic coupling may be involved in the mechanism of the action potential and that there should therefore be both consequent volume flows and pressure changes associated with such excitation. In a previous paper, such measurements were reported in cells of *Chara australis*, from which it is also known that during excitation there is an increase in KCl permeability and an efflux of KCl. In this paper, a number of theoretical analyses have been considered and developed pertaining to such measurements and the time-dependent relationships between apparent measured volume flows, true volume flows and turgor pressure changes in cells in various experimental situations. Such volume flows are quantitatively explained primarily from the frictional coupling of water by both K^+ and Cl^- ions and to a lesser extent by the local osmotic flow owing to KCl enhancement at the wall-membrane interface of the cell. The measured pressure changes of 12×10^{-3} to 28×10^{-3} atm during excitation are also correctly predicted as the result of such a volume outflow from the cell which behaves as a hydraulically leaky elastic cylinder and thereby drops in pressure. These conclusions then indicate that the volume flows and pressure changes measured are the incidental consequences of a change in membrane permeability and do not necessarily imply any electro-kinetic mechanism for the action potential itself.

In the preceding paper (Barry, 1970), which will henceforth be referred to as paper I, measurements were reported of both volume flows and pressure changes during electrical excitation in cells of the giant alga *Chara australis*. Such flows and pressure changes had, however, been predicted by various advocates of electro-kinetic models for the action potential (e.g., Teorell, 1958, 1959*a, b*, 1961, 1966; Kobatake & Fujita, 1964*a, b*). The question

* Present address: Physiological Laboratory, Downing Street, Cambridge, CB2 3EG, England.

then arises as to whether such measured flows and pressure changes do imply an electro-osmotic mechanism for the action potential or whether they would have occurred anyway, independent of any such model. This will be one of the main questions dealt with in this paper.

In the first part of this paper, relationships will be derived between measured and actual volume flows across membranes, and subsequent changes in turgor pressure of the cells, to determine any necessary corrections which have to be applied because of the experimental techniques used. Initially, the method of transcellular measurement of volume (primarily water) flow will be investigated in detail both for ordinary transcellular osmosis and for fast transient volume flows during an action potential. The first analysis will be considered not only as a check on the validity of the approach but also as a means of obtaining values of the volume elasticity constant of living *Characean* cells from the experiments of Kamiya and Tazawa (1966) on turgor pressure and volume changes during osmosis. The subsequent analysis will then indicate the relationship between the measured flow and the actual action potential flow.

In the latter part of this paper, theoretical predictions for both volume flows and pressure changes will be compared with those measured. Such predictions and calculations will then be used to determine whether the volume flows and pressure changes measured do imply one such electrokinetic feedback model for the action potential or whether they may simply be explained as the incidental consequences of a change in solute permeability during excitation.

All of the calculations in this paper were computed with a programmable Hewlett-Packard 9100A Calculator (Hewlett-Packard, Palo Alto, Calif.).

Volume Flows and Pressure Changes During Ordinary Transcellular Osmosis

In order to calculate the relationship between measured volume flow during ordinary transcellular osmosis and the true volume flow across the cell membranes, consider a cell held transcellularly, as in Fig. 1, so that the areas in compartments (1) and (2) are A_1 and A_2 , respectively. Then, if the solution in compartment (2) is changed to one of osmotic pressure π , there will be an outflow $J_2 > J_1$ and the cell will decrease in volume ($< 1\%$ for rigid plant cells), thus dropping in turgor pressure. The *change* in turgor pressure p will be related to the *change* in volume v of the cell (assuming that the cell deforms elastically; e.g., Kelly, Kohn & Dainty, 1963), by the

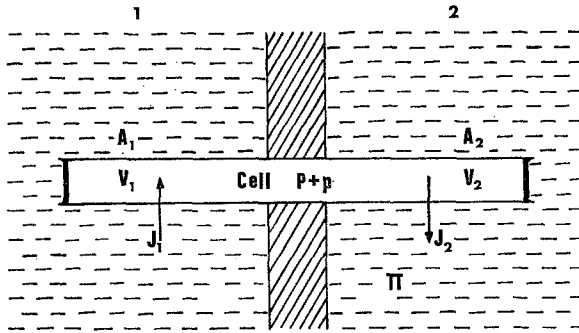


Fig. 1. A schematic diagram of the situation considered and used to calculate the total transcellular volume flow exactly and obtain an expression for the change in turgor pressure of the cell during transcellular osmosis. The cell is held transcellularly between two compartments. V_1 and A_1 represent the volume and area of that part of the cell in compartment 1, and similarly V_2 and A_2 for the cell in compartment 2. J_1 and J_2 refer to the respective flows in the directions indicated. π and P refer to the osmotic pressure of the external solution and the initial turgor pressure of the cell, respectively, whereas p refers to changes in the turgor pressure of the cell

equation

$$p = \frac{\epsilon v}{V_0} \tag{1}$$

where V_0 is the original volume and ϵ is the elastic modulus of the cell.

Since $dv/dt = (J_2 - J_1)$, the change in turgor pressure will then be given at any later time t by the equation

$$p = \int_0^t \frac{\epsilon}{V_0} (J_2 - J_1) dt. \tag{2}$$

Now

$$J_2 = L_{PX} A_2 (\pi - p) \tag{3}$$

and

$$J_1 = L_{PN} A_1 p \tag{4}$$

assuming that σ (the reflection coefficient of the membrane) is 1 for the solute under consideration, and where L_{PN} and L_{PX} , the endosmotic and exosmotic hydraulic conductivities of the membrane for inflows and outflows, respectively, are defined separately since Kamiya and Tazawa (1956) found experimentally that L_{PN} and L_{PX} are somewhat different in magnitude ($L_{PN}/L_{PX} \approx 1.6$). Hence, differentiating Eq. (2) and substituting for J_1 and J_2 ,

$$\frac{dp}{dt} = \frac{\epsilon}{V_0} L_{PX} A_2 \left[\pi - \frac{L_{PN} A_1 + L_{PX} A_2}{L_{PX} A_2} p \right]. \tag{5}$$

Integrating, since $p=0$ when $t=0$,

$$p = \frac{L_{PX} A_2}{L_{PN} A_1 + L_{PX} A_2} \pi (1 - e^{-\frac{t}{\tau_0}}) \quad (6)$$

where τ_0 represents the time constant for the cell turgor pressure to drop to

$\frac{L_{PX} A_2}{L_{PN} A_1 + L_{PX} A_2} \pi$ and is given by

$$\tau_0 = \frac{V_0}{\varepsilon(L_{PX} A_2 + L_{PN} A_1)}. \quad (7)$$

The total measured flow (i.e., the true volume flow into end 1 and the change in cell volume of end 1) is given by

$$J_1 + \frac{dV_1}{dt} = \frac{L_{PN} L_{PX} A_1 A_2 \pi}{L_{PN} A_1 + L_{PX} A_2} + L_{PX} A_2 \pi \left[\frac{V_1}{V_0} - \frac{L_{PN} A_1}{L_{PN} A_1 + L_{PX} A_2} \right] e^{-\frac{t}{\tau_0}} \quad (8)$$

from Eqs. (4)–(6), since

$$\frac{dV_1}{dt} = \frac{V_1}{V_0} \frac{dV}{dt} = \frac{d}{dt} \left(\frac{pV_1}{\varepsilon} \right) = \frac{V_1}{\varepsilon} \frac{dp}{dt}.$$

If $L_{PN} = L_{PX} = L_P$, A is proportional to V , and a negligible volume of the cell is in the stopper, then the second time-dependent term disappears and so the total measured flow is equal to the true osmotic flow $\frac{L_{PN} L_{PX} A_1 A_2 \pi}{L_{PN} A_1 + L_{PX} A_2}$ even though cell shrinkage is initially the main component of the total measured flow. This is equivalent to measuring the osmotic flow at effectively constant pressure. This of course does not take into account changes in osmotic pressure of the cell sap caused by the water flow. The same conclusion was also derived by Dainty and Ginzburg (1964) with the same implicit assumptions from an argument based purely on steady state flow rates.

Returning to a consideration of Eqs. (6) and (7), if $A_1 = A_2 = A$, and if the ratio of hydraulic conductivities $L_{PN}/L_{PX} = \rho$ (Kamiya & Tazawa, 1956) and represents the polarity in water permeability, then Eqs. (6) and (7) may be simplified since

$$L_{PX} = L_P \left(\frac{\rho + 1}{2} \right) \quad (9)$$

where L_P is the average hydraulic coefficient for a symmetrically partitioned cell. Therefore from Eq. (6)

$$p = \left(\frac{1}{\rho + 1} \right) \pi (1 - e^{-\frac{t}{\tau_0}}) \quad (10)$$

where

$$\tau_0 = \frac{2\rho V_0}{(\rho+1)^2 L_p \varepsilon A}. \quad (11)$$

Thus the final steady state change in turgor pressure of a cell under an overall osmotic gradient π is given by

$$p = \frac{\pi}{\rho+1}. \quad (12)$$

Now, from Eq. (1), the change in volume necessary to produce such a turgor pressure change is

$$\frac{v}{V_0} = \frac{p}{\varepsilon} = \frac{\pi}{\varepsilon(\rho+1)} \quad (13)$$

so that

$$\varepsilon = \frac{\pi}{(\rho+1)} \frac{V_0}{v}. \quad (14)$$

Tazawa and Kamiya (1966) have measured the change in volume after the onset of osmosis. It can be calculated from their data that one of their cells under an overall gradient of 8.13 atm after 1 min decreased in length by 0.136% and dropped in turgor pressure by 3.305 atm. Hence from Eq. (1), ε is 0.614×10^9 dynes \cdot cm $^{-2}$ (since 1 atm = 1.0132×10^6 dynes \cdot cm $^{-2}$), making the assumption as Kamiya and Tazawa did (based on Kamiya, Tazawa & Takata's 1963 experiments), that the relative volume change was approximately four times the relative change in length. From Eq. (12), these measurements give ρ a value of 1.51 which is fairly close to the average value they obtained directly, for different cells, of 1.6 (Tazawa & Kamiya, 1965). For the cells which they used, $L_p \approx 1.10 \times 10^{-5}$ cm \cdot sec $^{-1}$ \cdot atm $^{-1}$ (or 1.089×10^{-11} cm 3 \cdot sec $^{-1}$ \cdot dyne $^{-1}$) and a (avg.) ≈ 0.250 mm; assuming $\rho = 1.5$, and taking $\varepsilon = 0.6 \times 10^9$ dynes \cdot cm $^{-2}$.

$$\tau_0 = \frac{2\rho a}{\varepsilon(\rho+1)^2 L_p} = 1.79 \text{ sec.}$$

Therefore, *after* 5 sec, the turgor change should be about 94% of the total change, which compares with the observations Tazawa and Kamiya (1966) made that 80 to 90% of the total turgor change has been attained *within* the first 5 sec. This is good agreement considering possible uncertainties in ε , a and L_p .

These results, therefore, seem to verify the approach and its assumptions and give an estimate of the elastic modulus of the walls of about 0.6×10^9 dynes \cdot cm $^{-2}$, which is quite close to the range of values 0.2 to 0.4×10^9 dynes \cdot cm $^{-2}$ calculated (Appendix A) from the longitudinal modulus of

adult cells of *Nitella* obtained by loading the cell with a weight and measuring its extension (Kamiya *et al.*, 1963). Other measurements of ε for *Nitella* using length changes and half times for length changes, have been made by Kelly, Kohn and Dainty (1963). For external osmotic pressures σ between 0 and 5 atm, they reported values of ε between 200 and 600 atm. The true values are, however, approximately double these (J. Dainty *personal communication*) because in their paper they incorrectly assumed that γ_l (the longitudinal) and γ_r (the radial elastic moduli) were equal. This means that the experiments of Kelly *et al.* (1963) indicate that ε lies in the range 0.4 to 1.2×10^9 dynes \cdot cm $^{-2}$.

*Transcellular Volume Flows Resulting
from a Transient Volume Outflow at One End of a Cell*

Normally the cell was held transcellularly in the same experimental arrangement as described in the last section and one end of the cell stimulated. If volume flows accompany action potentials, such excitation should produce an outflow of solute and water, j , per unit area at that end. The measured transcellular volume flow may be derived in a similar manner to that derived in the last section except that, instead of an osmotic pressure gradient, there is a volume flow jA_2 out of the cell in compartment (2), during the action potential. In the actual calculations, j is considered as negative for a volume flow out of the cell. This will cause a drop p in the turgor pressure of the cell and a subsequent inflow of water J_1 and J_2 from each end of the cell. The total inflow J will, however, now be given by

$$J = J_1 + J_2 = L_{PN}(A_1 + A_2)p. \quad (15)$$

As before, the rate of change of pressure at any time, t , is given by

$$\frac{dp}{dt} = \frac{\varepsilon A_2}{V_o} \left(j - L_{PN} \frac{(A_1 + A_2)}{A_2} p \right) \quad (16)$$

where now the only hydraulic permeability involved is the endosmotic one L_{PN} . Since

$$L_{PN} = \frac{(\rho + 1)}{2} L_p \quad (17)$$

from Eq. (9) and the definition of " ρ ", then

$$\frac{dp}{dt} = \frac{\varepsilon A_2}{V_o} \left(j - \frac{(\rho + 1)(A_1 + A_2)}{2A_2} L_p p \right) \quad (18)$$

where $j = j(t)$ and $p = 0$ when $t = 0$.

The flow during an action potential is a continuous function which has a continuous derivative and hence may be represented by a Fourier series (Courant, 1937, pp. 439, 447). In fact, most of the contribution would come from a harmonic of frequency ω , related to the time t_m for the flow to reach a maximum by $\omega = \frac{\pi}{2t_m}$. As shown in Appendix C of paper I, the total flow $j(t)$ may be expressed in terms of a Fourier sine series as

$$j(t) = \sum_{n=0}^{n=\infty} j_{n\omega} \sin n\omega t = \text{Imaginary part} \sum_{n=0}^{n=\infty} j_{n\omega} e^{in\omega t}$$

where $i = \sqrt{-1}$.

For convenience, n will be dropped so that $j(t)$ will be written as $j(t) = \text{imaginary part} \sum_0^{\infty} j_{\omega} e^{i\omega t}$.

Hence Eq. (18) becomes

$$\frac{dp}{dt} = \frac{\epsilon A_2}{V_o} \left(\sum_0^{\infty} j_{\omega} \sin \omega t - \beta L_p p \right) \tag{19}$$

where

$$\beta = \frac{(\rho + 1)(A_1 + A_2)}{2A_2} \tag{20}$$

by definition. Eq. (19) is solved in Appendix B to give

$$p = \frac{\tau \epsilon A_2}{V_o} \sum_0^{\infty} j_{\omega} \cos \phi_{\omega} [\sin(\omega t - \phi_{\omega}) + \sin \phi_{\omega} e^{-\frac{t}{\tau}}] \tag{21}$$

where

$$\phi_{\omega} = \tan^{-1} \omega \tau \tag{22}$$

and

$$\tau = \frac{V_o}{\epsilon \beta L_p A_2}. \tag{23}$$

Now the observed flow (dV/dt) is the sum of the volume flow through end (1) and the change in volume (shrinkage) of end (1); i.e.,

$$\begin{aligned} & L_{PN} A_1 p + \frac{V_1}{\epsilon} \frac{dp}{dt}, \\ \therefore \frac{dV}{dt} &= L_{PN} A_1 \frac{\tau \epsilon A_2}{V_o} \sum_0^{\infty} j_{\omega} \cos \phi_{\omega} [\sin(\omega t - \phi_{\omega}) + \sin \phi_{\omega} e^{-\frac{t}{\tau}}] \\ &+ \frac{V_1 \tau \epsilon A_2}{\epsilon V_o} \sum_0^{\infty} j_{\omega} \omega \cos \phi_{\omega} \left[\cos(\omega t - \phi_{\omega}) - \frac{1}{\omega \tau} \sin \phi_{\omega} e^{-\frac{t}{\tau}} \right]. \end{aligned} \tag{24}$$

Since

$$L_{PN} = \frac{\rho + 1}{2} L_p = \frac{A_2 \beta}{A_1 + A_2} L_p,$$

Eq. (24) becomes (Appendix B)

$$\frac{dV}{dt} = \frac{A_1 A_2}{A_1 + A_2} j - \frac{\delta A}{A_1 + A_2} \cdot \frac{A_1 A_2}{A_1 + A_2} \sum_0^{\infty} j_{\omega} \sin \phi_{\omega} [\cos(\omega t - \phi_{\omega}) - \cos \phi_{\omega} e^{-\frac{t}{\tau}}] \quad (25)$$

where δA represents the area of the cell in the stopper.

As the fractional area of the cell in the stopper becomes very small; i.e., as

$$\frac{\delta A}{A_1 + A_2} \rightarrow 0 \quad \text{so} \quad \frac{dV}{dt} \cong \frac{A_1 A_2}{A_1 + A_2} j \quad (26)$$

and if also the cell is held symmetrically so that $A_1 = A_2 = A$, then

$$\frac{dV}{dt} \cong \frac{A}{2} j \quad (27)$$

so that the apparent measured volume flow is exactly half the true flow, and is not altered at all in shape or phase.

Normally, however, these conditions are not perfectly met and the apparent measured flow is slightly different from half the actual flows by the error term on the right side of Eq. (25). Actually the error introduced by the second term on the right side of Eq. (25) has been calculated for various values of τ for the main harmonics. It generally causes a delay of less than about 0.02 sec for cells longer than 5 cm with a stopper length of 1 cm. It also causes a reduction in magnitude of the flow, which is generally less than 15%.

This analysis has dealt with a volume outflow during excitation. If, however, an action potential was to cause an inflow, then the analysis would be very similar except that the error term of Eq. (25) is slightly modified as β must now be defined as

$$\frac{(\rho + 1)}{2\rho} \cdot \frac{(A_1 + A_2)}{A_2}$$

An Analysis of Turgor Pressure Changes Resulting from Uniform Transient Volume Flows

It will be assumed that the pressure change is purely caused by a volume outflow (primarily water), caused by some mechanism such as ion-water frictional coupling. It will be assumed that the cell is completely surrounded by a bathing solution and that the whole cell is stimulated instantaneously.

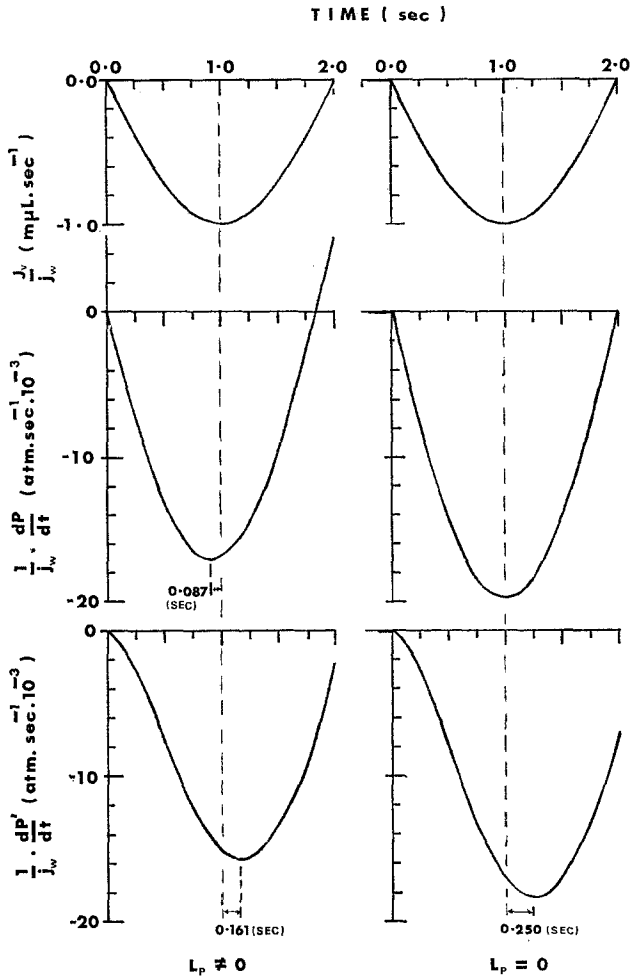


Fig. 2. The actual rate of change of turgor pressure, dP/dt (atm \cdot sec $^{-1} \times 10^{-3}$) and measured rate of change (owing to the time constant of the recording circuit), dP'/dt (atm \cdot sec $^{-1} \times 10^{-3}$) calculated for a cell during an action potential, for L_p finite and zero. This is shown as a function of time, t (sec), and is calculated [Eqs. (35), (45) & (48)] for $L_p = 1.0 \times 10^{-5}$ cm \cdot sec $^{-1} \cdot$ atm $^{-1}$ and $L_p = 0$. The elastic constant ϵ was taken as 0.6×10^9 dynes \cdot cm $^{-2}$ (or 5.92×10^2 atm), and the cell radius a as 0.06 cm. β was taken as 1.25 and the time constant of the recording circuit was 0.27 sec. This calculation assumed a sinusoidal volume flow J_v which reached a maximum in 1.00 sec. It was also assumed that the maximum value of the volume flow was 1.0 nliter \cdot sec $^{-1}$, and the values of dP/dt and dP'/dt corresponding to other values of j_ω may be obtained, as indicated, by multiplying by the numerical value of j_ω expressed in nliter \cdot sec $^{-1}$. Negative volume flow is an outflow, and a negative rate of change of pressure is a decrease in the rate of change of turgor pressure. The computed time delays of the maximum rate of change of pressure are also shown

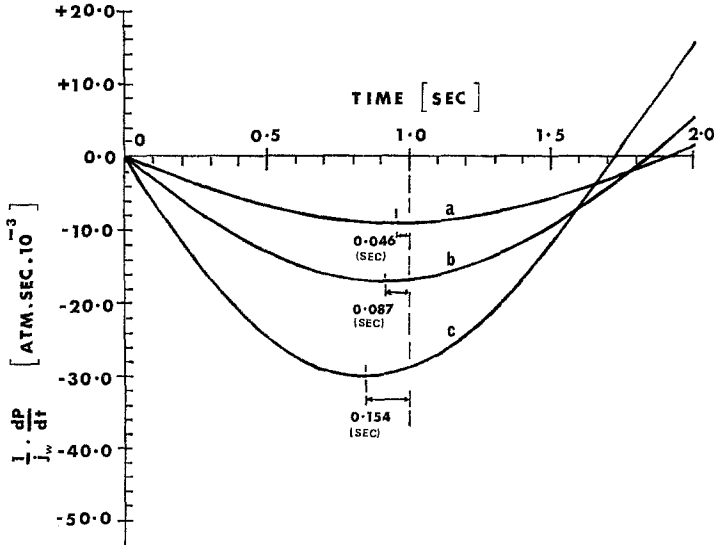


Fig. 3. The rate of change of turgor pressure dP/dt ($\text{atm} \cdot \text{sec}^{-1} \times 10^{-3}$) calculated for a cell during an action potential is shown as a function of time (sec) for various values of elastic constant ϵ ($\text{dynes} \cdot \text{cm}^{-2} \times 10^9$). $\epsilon = 0.3 \times 10^{-9}$ (curve a), 0.6×10^{-9} (curve b), and 1.2×10^{-9} (curve c) $\text{dynes} \cdot \text{cm}^{-2}$. The computed time delays of the maximum rates of change are also shown. These curves were calculated from Eq. (35) assuming a sinusoidal negative (outflow) volume flow with a maximum rate of $1.0 \text{ nliter} \cdot \text{sec}^{-1} \cdot \text{cm}^{-2}$ reached in 1 sec. They are also based on the assumption that $L_p = 1.0 \times 10^{-5} \text{ cm} \cdot \text{sec}^{-1} \cdot \text{atm}^{-1}$ and $a = 0.06 \text{ cm}$. Again a negative value of dP/dt is considered as a decrease in the rate of change of turgor pressure of the cell

The analysis will be the same as that of the previous section with the following modifications. The total volume flow will now be

$$J_{\text{total}} = L_{pN} A p \quad (28)$$

where A is now the area of the whole cell. The rate of change of pressure is now given by

$$\frac{dp}{dt} = \frac{\epsilon A}{V_o} \left[\sum_0^{\infty} j_{\omega} \sin \omega t - \beta L_p p \right] \quad (29)$$

where again $j(t)$ has been expanded in a Fourier sine series and now

$$\beta = \frac{\rho + 1}{2}. \quad (30)$$

Eq. (29) is identical to Eq. (19) if A is written for A_2 and β defined as in Eq. (30).

Hence the solution is

$$p = \frac{\tau \epsilon A}{V_o} \sum_0^{\infty} j_{\omega} \cos \phi_{\omega} \left[\sin(\omega t - \phi_{\omega}) + \sin \phi_{\omega} e^{-\frac{t}{\tau}} \right] \quad (31)$$

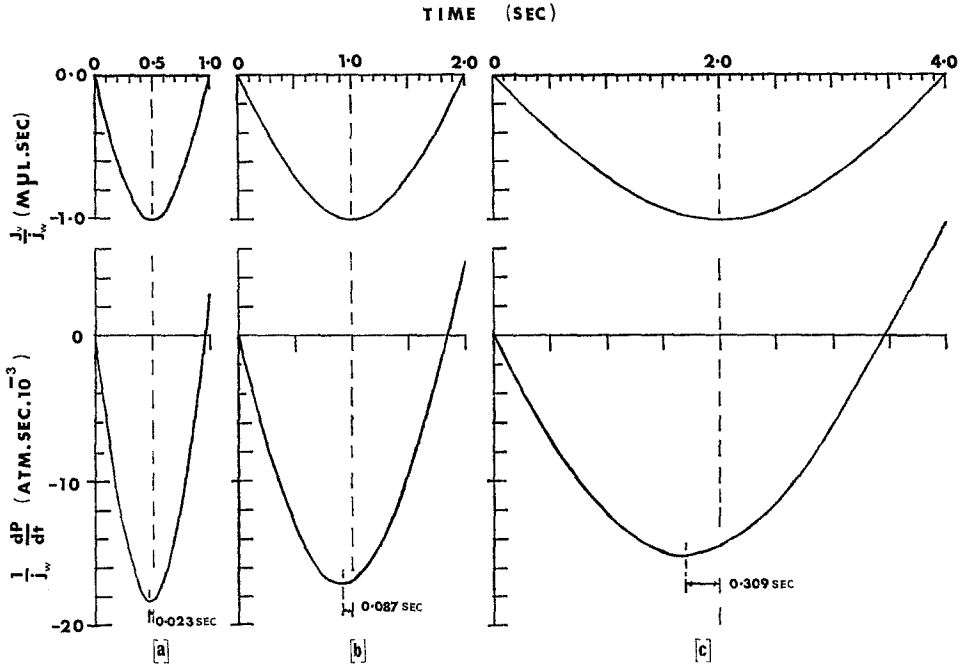


Fig. 4. The rate of change of turgor pressure dP/dt ($\text{atm}\cdot\text{sec}^{-1}\times 10^{-3}$) calculated for a cell during an action potential as a function of time for various frequencies, ω (radian $\cdot\text{sec}^{-1}$), of a sinusoidal volume flow J_v . $\omega = \pi$ (curve a), $\pi/2$ (curve b), and $\pi/4$ (curve c) radian $\cdot\text{sec}^{-1}$. The elastic constant ϵ was taken as 0.6×10^9 dyne $\cdot\text{cm}^{-2}$ (or 0.59218×10^3 atm) and the other parameters were the same as those mentioned for Fig. 3. The computed time delays of the maximum rates are also shown

where again

$$\phi_\omega = \tan^{-1} \omega \tau, \tag{32}$$

and now

$$\tau = \frac{V_o}{\epsilon \beta L_p A}. \tag{33}$$

Hence

$$\frac{dp}{dt} = \frac{\epsilon A}{V_o} \sum_0^\infty j_\omega \sin \phi_\omega [\cos(\omega t - \phi_\omega) - \cos \phi_\omega e^{-\frac{t}{\tau}}] \tag{34}$$

or

$$\frac{dp}{dt} = \frac{1}{\tau \beta L_p} \sum_0^\infty j_\omega \sin \phi_\omega [\cos(\omega t - \phi_\omega) - \cos \phi_\omega e^{-\frac{t}{\tau}}]. \tag{35}$$

Single harmonic contributions to dp/dt are plotted in Figs. 2 and 3 for various values of ϵ , and $\omega = \pi/2$ radians $\cdot\text{sec}^{-1}$ (assuming maximum flow reached in 1 sec) and in Fig. 4 for various values of ω .

Figs. 2-4 show the effect of hydraulic leakage in reducing the amplitude of the pressure change and causing a phase shift, advancing the peak of the rate of change of pressure.

*The Effect of the Finite Time Constant
of a Recording Circuit on Measured Pressure Transients*

Case I. Hydraulic leakage $L_p \neq 0$. The effect of the time constant of the recording circuit will now be analyzed. In particular, the effect of a filter condenser across (i.e., in parallel with) the chart recorder resistance will be examined.

Assuming a constant current source and an overall constant of proportionality K relating the cell's pressure to the current output,

$$i(t) = Kp(t). \quad (36)$$

Now

$$i_1 = C \frac{dV}{dt} \quad (37)$$

and

$$i_2 = \frac{V}{R} \quad (38)$$

where V is the voltage across the condenser, and i_1 is the current going through the condenser and i_2 that going through the chart recorder resistance. Hence

$$C \frac{dV}{dt} + \frac{V}{R} = i(t) = Kp \quad (39)$$

or

$$RC \frac{di_2}{dt} + i_2 = Kp. \quad (40)$$

But i_2 is the current going through the chart recorder and hence

$$p' = \frac{i_2}{K} \quad (41)$$

where p' is the uncorrected pressure calculated directly from the chart recorder output.

Hence it is related to the actual pressure p by

$$\frac{dp'}{dt} + \frac{p'}{\tau_2} = \frac{p}{\tau_2} \quad (42)$$

from Eqs. (40) and (41) where $\tau_2 = RC$ is the time constant of the recording circuit.

The solution of the homogeneous part of Eq. (42) is

$$p' = C_3 e^{-\frac{t}{\tau_2}} \quad (43)$$

where C_3 is an arbitrary constant.

Substituting for p from Eq. (31), Eq. (42) becomes

$$\frac{dp'}{dt} + \frac{p'}{\tau_2} = \frac{\varepsilon A}{V_o} \frac{\tau}{\tau_2} \sum_0^{\infty} j_{\omega} \cos \phi_{\omega} [\sin(\omega t - \phi_{\omega}) + \sin \phi_{\omega} e^{-\frac{t}{\tau}}]. \quad (44)$$

This is solved in Appendix C to give as the full solution

$$\begin{aligned} \frac{dp'}{dt} = \frac{1}{\beta L_p} \sum_{\omega} j_{\omega} \sin \phi_{\omega} & \left[\frac{\cos \theta_{\omega}}{\tau} \{ \cos(\omega t - \theta_{\omega} - \phi_{\omega}) - \cos(\theta_{\omega} + \phi_{\omega}) e^{-\frac{t}{\tau_2}} \} \right. \\ & \left. + \frac{\cos \phi_{\omega}}{(\tau_2 - \tau)} \{ e^{-\frac{t}{\tau}} - e^{-\frac{t}{\tau_2}} \} \right] \end{aligned} \quad (45)$$

where

$$\beta = \frac{\rho + 1}{2} \text{ [Eq. (30)], } \quad \tau = \frac{V_o}{\varepsilon \beta L_p A} \text{ [Eq. (33)],}$$

$$\phi_{\omega} = \tan^{-1} \omega \tau \text{ [Eq. (32)], and } \theta_{\omega} = \tan^{-1} \omega \tau_2 \text{ [Eq. (46)]}$$

where $\tau_2 = RC$ is the time constant of the recording circuit.

Eq. (45) has been used to calculate dp'/dt for single harmonics of j for different values of θ_{ω} and ϕ_{ω} , and a curve for one such harmonic with $\tau_2 = 0.27$ sec and other typical experimental parameters is shown in Fig. 2.

It effectively retards the peak of the signal by approximately τ_2 and slightly reduces the peak value for τ_2 small.

Case II. No hydraulic leakage, $L_p = 0$. If there is no leakage (i.e., $L_p = 0$), then

$$\frac{dp}{dt} = \frac{\varepsilon}{V_o} \frac{dV}{dt} = \frac{A\varepsilon}{V_o} \sum_{\omega} j_{\omega} \sin \omega t \quad (46)$$

from Eq. (29). Therefore, from Eqs. (42) and (46)

$$\frac{d^2 p'}{dt^2} + \frac{1}{\tau_2} \frac{dp'}{dt} = \frac{A\varepsilon}{V_o \tau_2} \sum_{\omega} j_{\omega} \sin \omega t. \quad (47)$$

As before, this may be solved for dp'/dt , with the condition that $dp'/dt = 0$ when $t = 0$, to give

$$\frac{dp'}{dt} = \frac{A\varepsilon}{V_o} \sum_{\omega} j_{\omega} \cos \theta_{\omega} [\sin(\omega t - \theta_{\omega}) + \sin \theta_{\omega} e^{-\frac{t}{\tau_2}}] \quad (48)$$

where again $\theta_{\omega} = \tan^{-1} \omega \tau_2$ as in Eq. (46).

Eqs. (46) and (48) have similarly been plotted (Fig. 2) for comparison with Eqs. (35) and (45) which take leakage into account.

It may be seen, in fact, for typical values of L_p and ε and for fast action potentials ($\tau_{\text{peak}} \leq 2.0$ sec), that the leakage has just the effect of advancing the time for the peak of the volume flow rate and slightly reducing its magnitude (Fig. 2).

An Analysis of the Volume Flow Caused by Local Concentration Enhancements in the Cell Wall During an Action Potential

There is a large efflux of solute across the plasmalemma during an action potential, and the solute will take a finite time to diffuse across the cell wall and into the external solution (e.g., Gaffey & Mullins, 1958). This enhanced local concentration at the membrane-wall interface would be expected to cause a local osmotic flow across the membrane.

The effect may be calculated as follows. Consider a cell (with an area of 1.0 cm^2) during an action potential transferring solute such as KCl from one side of the membrane to the other at a rate $\sum_{\omega} j_{\omega} \sin \omega t$, where j_{ω} is the value of the maximum rate of solute transported in $\text{mole} \cdot \text{sec}^{-1}$ for each harmonic of frequency ω .

For simplicity, only the main harmonic of frequency ω will be considered, where now $\omega = \frac{\pi}{2t_m}$ and t_m is the time taken for the action potential to reach its peak.

The following assumptions will be made to consider the effect for typical cylindrical *Chara* cells.

(1) The main contribution to the volume flow will be caused by concentration changes in the cell wall, since there D_{K^+} is about 2.5% of its free solution value (e.g., Gaffey & Mullins, 1958). Similarly D_{Cl^-} is about 0.25% of its free solution value (Mailman & Mullins, 1966) in the cell wall. Hence D_{KCl} will be between 5×10^{-7} and $5 \times 10^{-8} \text{ cm}^2 \cdot \text{sec}^{-1}$, and both values will be used in the calculations. The reduction in solute at the internal membrane-solution interface will be neglected since it will be much smaller owing to the higher value of D_{KCl} there.

(2) The cell wall will be considered as an infinite medium for short times, and no allowance will be made for the fact that it is finite and that the solute will diffuse much more quickly in the external solution. Provided $Dt/x^2 \lesssim 1$, this will give a reasonable estimate of the actual effect. Assuming, in fact, that $D \approx 5 \times 10^{-7}$ or $5 \times 10^{-8} \text{ cm}^2 \cdot \text{sec}^{-1}$, t is 2 sec and the cell wall is 10μ , then Dt/x^2 is in fact ≈ 1.0 or 0.1 , respectively.

(3) It will also be assumed that for simplicity the leakage of KCl back across the plasmalemma membrane may be neglected.

(4) For mathematical convenience, the equations and boundary conditions will be taken as similar to those for an enhancement at the interior of a cylinder of radius a . This is because of the extra difficulties encountered in considering the situation as being either the exterior of a cylinder, or

a plane surface in an infinite medium. For short times (less than 10 to 20 sec) and a diffusion constant $\leq 2 \times 10^{-5} \text{ cm}^2 \cdot \text{sec}^{-1}$, the difference between considering diffusion away from a plane interface and either a concave or converse surface of a cylinder of radius at least 0.5 mm is negligible. This has been checked for transport number calculations and is shown in Fig. 9 of Barry and Hope (1969a). Since the diffusion constants for KCl in the cell wall are at least two orders of magnitude smaller than the free solution values used in their calculations, and the times considered are less than 2 sec, this approximation is completely justifiable.

The diffusion equation is therefore:

$$\frac{\partial^2 c}{\partial r^2} + \frac{1}{r} \frac{\partial c}{\partial r} = \frac{1}{D} \frac{\partial c}{\partial t} \tag{49}$$

with the boundary condition

$$D \left(\frac{\partial c}{\partial r} \right)_a = j_\omega \sin \omega t \tag{50}$$

with c representing the *change* in concentration and being 0 for $t=0$ and with the condition that c is finite for $r=0$.

The above equations have been solved in Appendix D to give, at $r=a$,

$$c(a) = \frac{2j_\omega}{a\omega} + \frac{j_\omega}{2Di} \cdot \left[\frac{I_0 \left\{ a \left(\frac{i\omega}{D} \right)^{\frac{1}{2}} \right\} e^{i\omega t}}{\left(\frac{i\omega}{D} \right)^{\frac{1}{2}} \cdot I_1 \left\{ a \left(\frac{i\omega}{D} \right)^{\frac{1}{2}} \right\}} - \frac{I_0 \left\{ a \left(-i\frac{\omega}{D} \right)^{\frac{1}{2}} \right\} e^{-i\omega t}}{\left(-i\frac{\omega}{D} \right)^{\frac{1}{2}} \cdot I_1 \left\{ a \left(-i\frac{\omega}{D} \right)^{\frac{1}{2}} \right\}} \right] + 2 \sum_m j_\omega \frac{\omega e^{-D\alpha_m^2 t/a^2}}{a(D^2 \alpha_m^4/a^4 + \omega^2)} \tag{51}$$

where I_0 and I_1 refer to the hyperbolic Bessel functions of orders "0" and "1", respectively, $i^2 = -1$, $(\pm i)^{\frac{1}{2}} = \frac{i \pm 1}{2} = i^{\pm \frac{1}{2}}$, and α_m is a solution of $J_1(\alpha_m) = 0$.

Eq. (51) may be re-expressed in terms of the kindred Bessel functions M_0 and M_1 and θ_0 and θ_1 (see McLachlan, 1955, pp. 137-141). The complex part of the expression then disappears leaving

$$c(a) = 2j_\omega \left[\frac{1}{\omega a} + \frac{M_0[a\sqrt{\omega/D}]}{2\sqrt{\omega D} \cdot M_1[a\sqrt{\omega/D}]} \cdot \sin \left(\omega t + \theta_0[a\sqrt{\omega/D}] - \theta_1[a\sqrt{\omega/D}] + \frac{\pi}{4} \right) + \frac{\omega}{a} \sum_{m=1}^{\infty} \frac{e^{-D\alpha_m^2 t/a^2}}{(D^2 \alpha_m^4/a^4 + \omega^2)} \right] \tag{52}$$

For a uni-univalent electrolyte such as KCl, the volume flow will therefore be given by

$$J_v = 2\sigma L_p RTc(a). \quad (53)$$

Calculations

The volume flow was calculated assuming that the action potential reached a peak in 1.0 sec so that $\omega = \pi/2$ radian \cdot sec $^{-1}$. Two values of D were taken as 5.0×10^{-7} and 5.0×10^{-8} cm 2 \cdot sec $^{-1}$ \cdot atm $^{-1}$; a was taken as 0.05 cm and j_ω as $650 \times \pi/4 = 511$ pmole \cdot sec $^{-1}$ so that the net efflux given by $\int_0^\pi J_\omega \sin \omega t dt$, which is $2J_\omega/\omega$, was 650 pmoles.

The values of the Kindred functions were derived using the approximations

$$\text{Log}_{10} \left\{ \frac{M_0(z)}{M_1(z)} \right\} \approx 0.1536/z$$

and

$$\theta_0(z) - \theta_1(z) + \frac{\pi}{4} \approx -\frac{0.3534}{z} - 0.7854 \text{ radians}$$

Table. The volume flow J_v caused by local concentration enhancement in the cell wall during an action potential, shown as a function of time t . This assumed a sinusoidal KCl efflux as given below with a total efflux of 650 pmoles. The number of zeros of $J_1(\alpha_m)$ used to obtain a convergence of better than 10^{-8} between terms in the series expressions

$$\sum \frac{e^{-D\alpha_m^2 t/a^2}}{(\omega^2 + D^2\alpha_m^4/a^4)} \text{ is also given.}$$

t (sec)	0	0.25	0.5	0.75	1.0	1.25	1.5	1.75	2.0
Efflux (pmoles \cdot sec $^{-1}$)	0	187.9	347.1	453.5	490.9	453.5	347.1	187.9	0
J_v (nliter \cdot sec $^{-1}$) ^a	0.001 ^b	0.055	0.146	0.243	0.326	0.381	0.396	0.368	0.298
No. of terms used in series	2,254	149	111	93	82	75	69	64	61
J_v (nliter \cdot sec $^{-1}$) ^c	0.001 ^b	0.171	0.455	0.761	1.026	1.199	1.245	1.155	0.938
No. of terms used in series		380	289	245	218	198	184	172	163

^a $D_{\text{KCl}}(\text{cm}^2 \cdot \text{sec}^{-1}) = 5.0 \times 10^{-7}$.

^b This small rounding-off error may come from the approximations used in evaluating $M_0(z)/M_1(z)$ and $\theta_0(z) - \theta_1(z)$ and from cumulative rounding-off errors in the large numbers of values of α_m used.

^c $D_{\text{KCl}}(\text{cm}^2 \cdot \text{sec}^{-1}) = 5.0 \times 10^{-8}$.

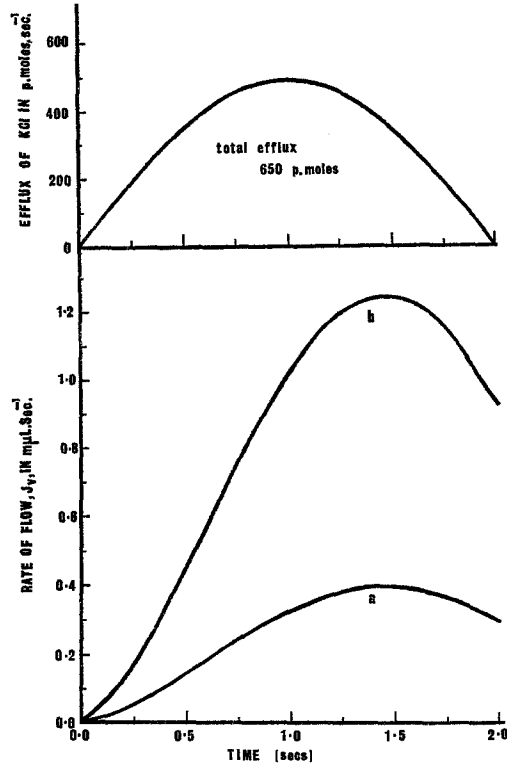


Fig. 5 (see table). The volume flow J_v (nliter \cdot sec $^{-1}$) caused by local concentration enhancement in the cell wall during an action potential, shown as a function of time t (sec). This assumed a sinusoidal KCl efflux (pmole \cdot sec $^{-1}$) (also shown in the figure) with a total efflux of 650 pmoles. The details of the calculation are discussed in the text

which were derived directly from the approximation formula given in McLachlan (1955, pp. 227, 228) for $z > 50$. In our case, $z \approx 89$ and 280 for $D = 5.0 \times 10^{-7}$ and 5.0×10^{-8} cm $^2 \cdot$ sec $^{-1}$, respectively. The first 40 values of the zeros of the equation $J_1(\alpha_m)$ were obtained from Watson (1944), and the rest were approximated by assuming that the difference $(\alpha_m - \alpha_{m-1}) \approx \pi$ (even after the first 40 terms $[(\alpha_m - \alpha_{m-1}) - \pi] < 0.0001$ or is $< 0.0001\%$ of α_m). The summation was continued until the difference between consecutive terms [of the whole last expression in Eq. (52)] was less than 10^{-8} ; the number of terms used in the computation are given in the Table. The results of these computations are given in the Table and shown in Fig. 5.

A Correlation of Theoretical Predictions and Experimental Results

The corrected average maximum rate of volume outflow for cells of *Chara australis* held transcellularly was found to be 0.88 ± 0.11 nliter \cdot sec $^{-1} \cdot$ cm $^{-2}$ (Barry, 1970).

Possible contributions to the volume flow

Since a cell in equilibrium has no net volume flow, J_v , across its membranes, the turgor pressure of the elastic wall, P , is balanced against the somotic pressure difference, Π_i , between the sap and the external solution, so that following Kedem and Katchalsky (1958).

$$J_v = 0 = L_p(P - \sigma(\Pi_i - \Pi_o)) \quad (54)$$

where σ , the reflection coefficient of the membranes to the salt solution (mainly KCl), is approximately 1.0 in the *resting* state. During excitation there are changes in solute permeability, ω , [P_{KCl} in particular increases (Hope & Findlay, 1964) and therefore P_{KCl} will increase) σ , and also $\Delta\Pi$ (i.e., $\Pi_i - \Pi_o$) and P . In this transient state, the volume flow outwards will be given approximately by

$$J_t = J_v - L_p \delta P = L_p \delta \sigma \Delta\Pi + L_p \sigma \delta(\Delta\Pi) - L_p \delta P \quad (55)$$

where J_t refers to the total transient volume flow and J_v that resulting directly from the action potential; $\delta\sigma$ refers to a decrease in the reflection coefficient, $\delta(\Delta\Pi)$ to a drop in the effective local osmotic pressure across the cell membranes themselves, and δP to a decrease in turgor pressure resulting from the volume flow itself. When the volume flow is measured transcellularly, however, this feedback caused by the pressure change itself is not measured. The reasons are completely analogous to the analysis and discussion surrounding Eq. (8).

Since the reflection coefficient may be related to the solute permeability, ω , by an equation of the form

$$\sigma = 1 - \frac{\omega \bar{V}_s}{L_p} - \omega \chi_{13} \quad (56)$$

similar to that given by Katchalsky and Kedem (1962), where the solute permeability ω (moles $\text{cm}^{-2} \text{sec}^{-1} \cdot \text{atm}^{-1}$) is related to the more conventional solute permeability coefficient P_s ($\text{cm} \cdot \text{sec}^{-1}$) by

$$P_s = \omega RT \quad (57)$$

where \bar{V}_s is the partial molar volume of the solute and χ_{13} refers to their term representing frictional drag of the solute (in this case, ions) on the water.

During excitation, therefore, the change in reflection coefficient, $\delta\sigma$, may be related to the change in solute permeability, $\delta\omega$, by

$$\delta\sigma = -\frac{\bar{V}_s}{L_p} \delta\omega - \delta(\omega \chi_{13}). \quad (58)$$

¹ This equation tacitly assumes that $L_{PX} = L_{PN} = L_P$, or that $\beta = 1$.

The contribution of this change in reflection coefficient to the volume flow, J_σ , out of the cell is from Eqs. (55) and (58)

$$J_\sigma = L_p \frac{\bar{V}_s \delta \omega}{L_p} \Delta \Pi + L_p \delta(\omega \chi_{13}) \Delta \Pi. \quad (59)$$

Since the second term on the right side refers only to ion-water frictional interaction in the membrane, it may be replaced by the term $\bar{V}_w \alpha \Psi_s$, where Ψ_s is the flux of solute (e.g., in moles · unit area⁻¹ · sec⁻¹), α is the frictional coupling coefficient (e.g., in moles of water · mole of ions⁻¹) and \bar{V}_w is the partial molar volume of water, so that Eq. (59) thus becomes

$$J_\sigma = \bar{V}_s \delta \omega \cdot \Delta \Pi + \bar{V}_w \alpha \Psi_s. \quad (60)$$

Since, however,

$$\Delta \Pi \simeq RT \Delta C_s \quad (61)$$

and

$$\Psi_s \simeq \delta \omega RT \Delta C_s, \quad (62)$$

Eq. (60) may be written as

$$J_\sigma = (\bar{V}_s + \alpha \bar{V}_w) \delta \omega \cdot RT \Delta C_s \quad (63)$$

an equation showing that the flow owing to a change in the reflection coefficient is, as expected, composed of two terms: the first just owing to the volume of solute moving and the second to the volume of water being frictionally dragged with that solute. Hence Eq. (55) may be written in the form

$$J_t = (\bar{V}_s + \alpha \bar{V}_w) \delta \omega \cdot RT \Delta C_s + \sigma L_p \delta(\Delta \Pi) - L_p \delta P \quad (64)$$

or from Eq. (62)

$$J_t = (\bar{V}_s + \alpha \bar{V}_w) \Psi_s + \sigma L_p (\Delta \Pi) - L_p \delta P. \quad (65)$$

Eq. (64) shows that changes in σ and $\Delta \Pi$ will tend to cause a volume outflow and are, for the case considered in this paper, caused by changes in reflection coefficient (excluding the frictional drag component), ion-water frictional interaction, and local concentration enhancement in the cell wall. As already shown, the first two contributions are in fact both parts of the full thermodynamic reflection coefficient, and have been kinetically separated to give greater insight into the mechanism of volume flow. In general, the change in P resulting from this volume flow will then tend to feed back to cause a reduction in the volume flow, but, as we discussed on p. 338, the transcellular method of measurement actually measures the volume outflow at effectively constant pressure. The contribution of each of these components will now be considered in more detail.

*Change in Reflection Coefficient
(Excluding the Ion-Water Frictional Coupling Term)*

The contribution of this term has already been shown to be $\bar{V}_s \Psi_s$ from Eq. (65), where Ψ_s is the rate of efflux of KCl at the peak of the action potential.

However, Hope and Findlay (1964) and Coster (M. Sc. thesis, Univ. of Sydney, 1964) have both measured chloride effluxes from *Chara australis* during an action potential. Hope and Findlay found a net loss of about 500 pmoles \cdot cm⁻² \cdot action potential⁻¹ of chloride for *Chara australis*. They obtained this value directly from chloride flux experiments. Coster obtained a value for the net chloride efflux in a cell of *Chara australis* of about 800 pmoles \cdot cm⁻² \cdot action potential⁻¹. He calculated this from the change in Cl⁻ activity in the cytoplasm during excitation measured with a Ag-AgCl electrode. An average figure of 650 \pm 150 pmoles \cdot cm⁻² \cdot action potential⁻¹ will be taken for the following calculation. If it is further assumed that this efflux is composed mainly of a dominant sinusoidal harmonic of 1/4 period = 1 sec, similar in time course to the potential transients observed, the rate of efflux at the peak of the action potential Ψ_s , will be related to the total efflux of KCl, Φ_s , by

$$\Psi_s = \frac{\pi}{4} \Phi_s$$

so that $\Psi_s = 511$ pmoles \cdot cm⁻² \cdot sec⁻¹ (*cf.* the top graph of Fig. 5, calculated for a total efflux of 650 pmoles \cdot cm⁻² \cdot sec⁻¹). Since $\bar{V}_s = 26.7$ cm³ \cdot mole⁻¹ (Wirth, 1937), the contribution of this term will therefore only be

$$= 13.6 \times 10^{-9} \text{ cm}^3 \cdot \text{cm}^{-2} \cdot \text{sec}^{-1}$$

or

$$\simeq 0.014 \text{ nliter} \cdot \text{cm}^{-2} \cdot \text{sec}^{-1}.$$

Ion-Water Frictional Interaction

Since both K⁺ and Cl⁻ ions move out together during an action potential, it would seem only logical that both will make a contribution to the water dragged by frictional interaction. This is almost equivalent to electrokinetic drag except that here we have no current and both K⁺ and Cl⁻ ions are moving in the same direction. It will therefore be assumed that the coefficient is the same for both ion species, and equal to the cation electro-osmotic coefficient in the resting state so that the contribution to Ψ_s in Eq. (65) will be double the electro-osmotic coefficient measured in the non-excited state for positive ions alone. Using the figure of 5.8 μ liters \cdot

coulomb⁻¹ (Barry & Hope, 1969 *c*), which implies that each ion drags with it about 31 moles of water, for the electro-osmotic coupling coefficient and the figure of 511 pmoles·cm⁻²·sec⁻¹ for the peak rate of KCl efflux calculated in the previous section, the contribution of this component J_e to the total volume flow rate from Eq. (65) will be given by

$$J_e = 18 \times 2 \times 31 \times 511 \times 10^{-12} \text{ cm}^3 \cdot \text{cm}^{-2} \cdot \text{sec}^{-1}$$

so that

$$J_e = 0.57 \text{ nliter} \cdot \text{cm}^{-2} \cdot \text{sec}^{-1}.$$

Local Concentration Enhancement

The third possible contribution is similar in principle to the flows caused by local concentration enhancement during the transport number effect (Barry & Hope, 1969 *a, b*). The volume flow, likely to be caused by such local concentration enhancement in the cell wall during an action potential, was calculated as stated on pp. 348–351. Two possible values of D_{KCl} (wall) were taken as 5.0×10^{-7} and 5.0×10^{-8} cm²·sec⁻¹ with the other parameters the same as in the previous sections.

The results are shown in Fig. 5 for a postulated sinusoidal action potential. These were calculated for an efflux of 650 pmoles of KCl. As indicated in Fig. 5 and the Table, the maximum rates of flow will be 0.42 and 1.3 nliter·sec⁻¹ for diffusion constants of 5×10^{-7} and 5×10^{-8} cm²·sec⁻¹, respectively. There is, however, a time delay of about 0.5 sec in both cases between the peak of the action potential flux and the predicted flow maximum, so that the actual contribution of this component after 1 sec, at the peak of the action potential, will only be between 0.34 and 1.1 nliter·cm⁻²·sec⁻¹ for the two values of D_{KCl} chosen. However, the close correlation of the time course of the observed volume flows with the action potential curves, which will be further discussed in the section on time courses, precludes the possibility that this component is making a dominant contribution to the total volume flow.

Summary

It would seem that the primary contribution to the volume flow would be from the ion-water frictional coupling; e.g., for an efflux of about 650 pmoles of KCl per cm², the contribution of the frictional coupling would be about 0.57 nliter·sec⁻¹·cm⁻².

The secondary contribution would be about $0.01 \text{ nliter} \cdot \text{sec}^{-1} \cdot \text{cm}^{-2}$ for the solute flow part of the change in reflection coefficient, and up to $0.34 \text{ nliter} \cdot \text{sec}^{-1} \cdot \text{cm}^{-2}$ or higher, depending on the value of the diffusion constant in the cell wall, D_{KCl} , for local KCl enhancement in the wall.

The feedback contribution produced by the drop in pressure itself during the action potential is not part of the volume flow measured in transcellular experiments. Hence the total calculated volume flow for a KCl efflux of $650 \text{ pmoles} \cdot \text{cm}^{-2}$ is up to about $0.92 \text{ nliter} \cdot \text{sec}^{-1} \cdot \text{cm}^{-2}$ or so. Thus the calculated flows agree well with the corrected experimental flows of about $0.88 \pm 0.11 \text{ nliter} \cdot \text{sec}^{-1} \cdot \text{cm}^{-2}$.

Time Course

The correction for using a stopper of a finite length [Eq. (25)] should be taken into account when an analysis of the time course of the flows is being made. This was found to cause a delay of approximately 0.01 to 0.02 sec for the cells used, and, as may be seen from the corrected values for the maximum rate of volume flows shown in Table 1 of paper I, the average maximum rate of volume flow lagged behind the action potential peak by $0.17 \pm 0.08 \text{ sec}$.

Thus in these measurements, the volume flow followed the time course of the action potential (i.e., the sum of both the plasmalemma and tonoplast action potentials) very closely. This is in contrast with the results of Kishimoto and Ohkawa (1966), who recorded a delay of almost 2 sec between their action potential peak and their apparent maximum rate of volume flow. Both this time lag and the very low magnitude of their volume flows (approximately 1/10 of the magnitude of those obtained by the author for *Chara* and by Fensom (1966) for *Nitella*) suggest that the inertia of their system is a limiting factor in their experiments (with a time constant of the order of 5 sec).

Pressure Measurements During an Action Potential and Their Relationship to Volume Flow

From the value of ε of $0.6 \times 10^{-9} \text{ cm}^2 \cdot \text{dyne}^{-1}$ obtained from the experiments of Tazawa and Kamiya (1966) on *Nitella flexilis*, and from the action potential volume flows already mentioned, Eq. (35) and Figs. 2 and 3 would predict maximum rates of change of pressure from about 13×10^{-3} to $21 \times 10^{-3} \text{ atm} \cdot \text{sec}^{-1} \cdot \text{cm}^{-2}$ of cell area. These should be compared with rates of change of pressure determined experimentally of 9×10^{-3} to $62 \times 10^{-3} \text{ atm} \cdot \text{sec}^{-1} \cdot \text{cm}^{-2}$ of cell area (see Table 2 of paper I).

The validity of using such a value of ε is further supported by the agreement of the predicted time lead of the *actual* pressure rate peak of +0.02 to +0.31 sec (Fig. 4, considering values of τ_{ap} varying from 0.5 to 2.0 sec) with the experimentally determined ones (Table 2 of paper I) of -0.8 to +0.6 with an average value of $+0.09 \pm 0.07$. A decrease in ε from the value assumed would increase the time lead and the magnitude of the pressure change as indicated in Fig. 3.

Thus the turgor pressure change may simply be explained as the result of the volume outflow from a leaky elastic cell wall cylinder enclosing a membrane.

*Discussion of Electrokinetic Models for the Action Potential
in the Light of the Measurements of Volume Flow
and Pressure Changes Made during Them*

The Teorell Model. Teorell (1958, 1959*a, b*, 1962) has proposed an electro-osmotic model for the action potential. He considers the five following equations as the basis of his membrane-oscillator model:

$$V = -SP + \ell E \text{ (electro-osmotic flow velocity equation),} \quad (66)$$

$$E = IR \text{ (Ohm's law),} \quad (67)$$

$$R^\infty = f(V) \text{ (resistance-flow velocity relation),} \quad (68)$$

$$\frac{dR}{dt} = K(R^\infty - R) \text{ (time delay function),} \quad (69)$$

and

$$V = q \frac{dP}{dt} \text{ (geometry requirement)} \quad (70)$$

where V is the water flow velocity, S the hydraulic permeability, ℓ the electro-osmotic permeability constant, R^∞ the steady state resistance, q a constant dependent on the geometry of the system, K a constant parameter, with the other terms already defined.

In a later modification of his model (e.g., Teorell, 1966), he includes two further equations to take into account hydraulic leakage via an additional water pathway. However, the essential features of his model can be understood by considering Eqs. (66)–(70) and are as follows. Initially the concentration profile through the membrane is linear. Then, as a stimulating current passes through the membrane, the resulting electro-osmotic flow will cause the concentration to decrease to form a concave profile. This will cause an increase in resistance resulting in an increase in the change in p.d.

caused by the current pulse itself. This increase in p.d., he says, should then in turn increase the electro-osmotic flow. This volume flow will, however increase the pressure difference [Eq. (70)] until it equals the electro-osmotic force, thus causing the flow to drop to zero. Then diffusion will cause the profile to change back towards a linear profile as indicated by Eq. (69). This would cause the electro-osmotic component to decrease and the p.d. would drop in turn.

The Kobatake-Fujita Model. A similar model has also been proposed by Kobatake and Fujita (1964*a, b*). They, however, formulated the electro-kinetic coupling in a different way and proposed a different restoring force.

They considered the physical situation inside a capillary and wrote down the hydrodynamic Navier-Stokes equation for the equation of motion. This related the velocity at each point with the pressure, potential and concentration. They considered a fixed-charge concentration at the internal surface of each capillary and, assuming the applicability of the Boltzmann equation, calculated the charge distribution inside each pore. This distribution was incorporated into their original equation of motion. Then using conservation of mass and charge equations, together with the pressure change caused by the water flow into the external chambers, they showed that such a system could be stimulated to cause an oscillatory phenomena with this pressure as the restoring force.

Objections to Both Models. Qualitatively the sequence of events suggested by Teorell's model outlined above differs from the situation found in *Chara* cells where, *if there were changes* in the concentration profile in the membrane, the depolarizing pulse would tend to cause the profile to become more convex. On Teorell's model, this would decrease the resistance and instead of increasing the p.d. would decrease it, therefore producing a negative rather than a positive feedback required at the onset of an action potential.

Also in Eq. (66), Teorell (e.g., 1958, 1966) does not consider possible changes in reflection coefficient and assumes that the electro-osmotic coupling coefficient as he defines it is constant. If both cations and anions contribute to the ion-water coupling during excitation, any electro-osmotic movement will considerably underestimate the water flow dragged by both ion species.

In defense of Teorell's model, it should be said that he has an artificial membrane oscillator (Teorell, 1959*a*, 1962) which does obey all his equations and exhibits concomitant volume flows and pressure changes during action potentials. However, justification is still needed for the application of the resistance-flow velocity relation and the restoring force equation [Eqs. (68)

and (69)], which hold for his 7,000-Å pores, to biological membranes with cation pores or channels, where anions tend to be excluded and concentrations are not likely to change significantly.

Kobatake and Fujita's (1964*a, b*) model, on the other hand, neglects hydraulic leakage and also suffers, as far as its application to biological membranes is concerned, since it requires large pores as well.

Neither model as it stands can explain the transient increase in anion conductance during excitation, and would require further modification to take such an effect into account.

Discussion

In both the models of Teorell and of Kobatake and Fujita, the basic mechanism proposed for the action potential hinges on a change in pore concentration, owing to electro-osmosis, followed by a change in electro-osmosis again to give a positive feedback system. Although these models have been of value in suggesting the presence of volume flows and pressure changes accompanying action potentials, neither in its present form appears to be applicable to giant algal cells.

However, the semi-empirical equations, which certainly do apply for volume flow in plant cells during excitation, may be written as follows.

$$J_t = J_v - L_p p = (\bar{V}_s + \alpha \bar{V}_\omega) RT \Delta C_s \cdot \delta \omega + \alpha L_p RT \cdot \delta (\Delta C_s) - L_p p \quad (71)$$

$$\frac{dp}{dt} = \frac{\epsilon A}{V_o} (J_v - L_p p) \quad (72)$$

where these equations are equivalent to Eqs. (64) and (29) and where the symbols are as previously defined.

There would seem to be two possible mechanisms for the transient nature of the action potential.

Pressure-Volume Flow Feedback System

In this case, the pressure might be considered as a restoring force interacting with the volume flow to cause a positive feedback oscillatory system if the change in solute permeability (e.g., Cl^- permeability), was itself a particular function, $F(J_t)$, of the total volume flow.

That is, if

$$\delta \omega = F(J_t) \quad (73)$$

such that

$$\frac{dF}{dJ_t} > 0 \quad \text{but} \quad \frac{d^2F}{dJ_t^2} < 0$$

with

$$F(J_t) = 0 \quad \text{when} \quad J_t = 0$$

as, for example,

$$\delta \omega = \delta \omega_0 (1 - e^{-J_t/k})$$

where $\delta \omega_0$ and K are constants, then Eqs. (71) and (72) combined with Eq. (73) would constitute a feedback system of equations capable of producing oscillations in solute permeability, volume flow and turgor pressure, provided the system was initiated, for example, by an electro-osmotic water flow in the appropriate direction. If this was the true mechanism, it would also differ from the other models in that it does not require the choice of any particular electro-osmotic model.

An Independent Solute Permeability System

If there was no coupling between volume flows and solute permeability, then the observed transient oscillation in both pressure and volume flow could still be the natural result of an unrelated transient change in solute permeability as discussed so far in this paper. This would be the case if the permeability change was either part of, or resulted from, a closed electro-structural feedback loop.

In conclusion, it may be said that during an action potential there is a volume outflow of about $3 \text{ nliter} \cdot \text{cm}^{-2}$, with a peak rate of about $0.88 \pm 0.11 \text{ nliter} \cdot \text{cm}^{-2} \cdot \text{sec}^{-1}$ (Paper I), which is primarily caused by ion-water interaction coupling and to a lesser extent by local osmosis owing to the efflux of KCl, itself resulting from a transient increase in effective KCl permeability (primarily owing to an increase in Cl^- permeability).

There is also a pressure change measured as about 12 to $26 \times 10^{-3} \text{ atm}$ with a peak rate of 9 to $36 \times 10^{-3} \text{ atm} \cdot \text{sec}^{-1}$. This is caused by the volume outflow from the cell, which behaves as a leaky elastic cylinder ($\epsilon \approx 0.6 \times 10^9 \text{ dynes} \cdot \text{cm}^{-2}$), and thereby drops in pressure.

Although, as predicted by the various electro-kinetic models, there are volume flows and pressure changes during action potentials in plant cells, the calculations and discussions given in this paper indicate that such volume flows and pressure changes may be incidental consequences of a change in membrane potential and do not necessarily imply an electro-kinetic mechanism for the action potential itself.

These results indicate that volume flow and pressure changes may well be the mechanisms for the action of some plants and give some teleological reason for the presence of the action potential at least in some plants, e.g., *Venus fly trap*, *Mimosa* and *Eloedea*. In particular, Allen (1969) has shown that there is a large efflux of K^+ from the cells in the "active region" of *Mimosa* and proposed some transient change in their semi-permeability as the cause for a loss in turgor.

I am indebted to Professor A. B. Hope, my former Ph. D. supervisor, for helpful advice and encouragement during this work. I would also like to thank Drs. J. Dainty, R. S. Eisenberg and E. M. Wright for their helpful critical readings of the manuscript.

I was the holder of research studentships from the Australian Commonwealth Scientific and Industrial Research Organization (C.S.I.R.O.) and Flinders University during the course of most of this work, which was carried out at both the University of Sydney and Flinders University, and is included in part III of a Ph. D. thesis (Barry, 1967). The work was also supported in part at the University of California at Los Angeles by Public Health Service Grant GM 14772.

Appendix A

To Derive an Expression Relating the Longitudinal Modulus of Elasticity with the Volume Modulus Defined by Eq. (1) for the Whole Cell

The actual tensions per unit area in the wall owing to the pressure inside the cell may easily be shown to be given by (e.g., Kamiya, Tazawa & Takata, 1963):

$$T_l = \frac{Pa}{2d} \quad (\text{A.1})$$

$$T_t = \frac{Pa}{d} \quad (\text{A.2})$$

where T_l and T_t are the longitudinal and transverse tensions per unit area, P is the turgor pressure of the cell, a is the radius and d is the thickness of the wall.

By definition, the longitudinal and transverse elastic moduli (γ_l and γ_t) are given by Tazawa and Kamiya (1965) as

$$\frac{\Delta \ell}{\ell} = \frac{1}{\gamma_l} (T_l - \sigma T_t) \quad (\text{A.3})$$

and

$$\frac{\Delta a}{a} = \frac{1}{\gamma_t} (T_t - \sigma T_l) \quad (\text{A.4})$$

where ℓ is the length of the cell, $\Delta \ell$ and Δa are the changes in length and radius and σ is the "apparent" Poisson's ratio (defined as the ratio of the fractional change in width to the fractional change in length when a strip of cell wall is stretched).

Since the volume of the cell, V , is given by

$$V = \pi a^2 \ell, \quad (\text{A.5})$$

then

$$\frac{\Delta V}{V} = \frac{2\Delta a}{a} + \frac{\Delta \ell}{\ell} \quad (\text{A.6})$$

for small changes in volume.

Substituting from Eqs. (A.1)–(A.4)

$$\frac{\Delta V}{V} = \frac{Pa}{d\gamma_t} \left\{ \frac{4 + \beta - 2\sigma(1 + \beta)}{2\beta} \right\} \quad (\text{A.7})$$

where β has been defined as the ratio of γ_c/γ_t .

From the definition of ε from Eq. (A.1),

$$P = \varepsilon \frac{\Delta V}{V}.$$

Comparing with Eq. (A.7),

$$\varepsilon = \frac{2\beta d}{a} \frac{\gamma_t}{[(4 + \beta) - 2\sigma(1 + \beta)]}. \quad (\text{A.8})$$

Kamiya *et al.* [(1963) (for a fully grown cell of *Nitella flexilis*, $d = 7.7 \times 10^{-3}$ mm, $a = 0.195$ mm)] found that, by stretching this cell with appropriate weights, its longitudinal modulus of elasticity varied between 4 and 7×10^9 dynes \cdot cm $^{-2}$. Tazawa and Kamiya (1965) have calculated from the data of the previous authors that $\beta = 3.3$ and $\sigma = 0.3$. Substituting all these values into Eq. (A.8) gives ε as between 0.2 and 0.4×10^9 dynes \cdot cm $^{-2}$.

Appendix B

The Solution of the Equation Relating Measured Volume Flow with Actual Volume Flow

To solve Eq. (19),

$$\frac{dp}{dt} = \frac{\varepsilon A_2}{V_o} \left(\sum_0^{\infty} j_{\omega} \sin \omega t - \beta L_p p \right) \quad (\text{B.1})$$

where $p = 0$ when $t = 0$.

Rewriting in terms of exponentials and only considering the imaginary part of the particular solution, Eq. (B.1) becomes

$$\frac{dp}{dt} = \frac{\varepsilon A_2}{V_o} \left(\sum_0^{\infty} j_{\omega} e^{i\omega t} - \beta L_p p \right). \quad (\text{B.2})$$

The solution of the homogeneous equation may be written down immediately as

$$p = C_1 e^{\frac{-t}{\tau}} \quad (\text{B.3})$$

where C_1 is an arbitrary constant and

$$\tau = \frac{V_o}{\varepsilon \beta L_p A_2}. \quad (\text{B.4})$$

The particular solution of Eq. (B.4) may be obtained by trying a trial solution

$$p = \sum_0^{\infty} C_{\alpha} e^{\alpha t} \quad (\text{B.5})$$

where C_{α} and α are constants to be determined. Substituting into Eq. (B.4), this becomes

$$\sum \alpha C_{\alpha} e^{\alpha t} = \frac{\varepsilon A_2}{V_o} (\sum j_{\omega} e^{i\omega t} - \beta L_p \sum C_{\alpha} e^{\alpha t}).$$

Since this must be identically true for all t , each α must equal $i\omega$ and hence

$$C_{\alpha} \left(i\omega + \frac{1}{\tau} \right) = \frac{\varepsilon A_2 j_{\omega}}{V_o} \quad (\text{B.6})$$

$$\therefore C_{\alpha} = \frac{\varepsilon A_2 \tau j_{\omega}}{V_o (1 + i\omega\tau)}.$$

Therefore the particular solution is

$$p = \text{Imaginary part} \left[\frac{\varepsilon A_2 \tau}{V_o} \sum \frac{j_{\omega} e^{i\omega t}}{(1 + i\omega\tau)} \right]; \quad (\text{B.7})$$

i.e.,

$$p = \frac{\tau A_2 \varepsilon}{V_o} \sum_{\omega=0}^{\infty} j_{\omega} \left[\frac{1}{\sqrt{1 + (\omega\tau)^2}} \cdot \frac{\sin \omega t - \omega\tau \cos \omega t}{\sqrt{1 + (\omega\tau)^2}} \right] \quad (\text{B.8})$$

or

$$p = \frac{\tau A_2 \varepsilon}{V_o} \sum j_{\omega} \cos \phi_{\omega} (\sin \omega t \cos \phi_{\omega} - \cos \omega t \sin \phi_{\omega}) \quad (\text{B.9})$$

where $\phi_{\omega} = \tan^{-1} \omega\tau$.

Using the trigonometrical identities (e.g., Comrie, p. 380, 1955),

$$p = \frac{\tau A_2 \varepsilon}{V_o} \sum j_{\omega} \cos \phi_{\omega} \sin(\omega t - \phi_{\omega}). \quad (\text{B.10})$$

Therefore the full solution is

$$p = \left[\frac{\tau A_2 \varepsilon}{V_o} \sum_{\omega=0}^{\infty} j_{\omega} \cos \phi_{\omega} \sin(\omega t - \phi_{\omega}) \right] + C_1 e^{-\frac{t}{\tau}}. \quad (\text{B.11})$$

Since, however, $p=0$ when $t=0$,

$$C_1 = -\frac{\tau A_2 \varepsilon}{V_o} \sum j_{\omega} \cos \phi_{\omega} \sin \phi_{\omega}.$$

Hence

$$p = \frac{\tau A_2 \varepsilon}{V_o} \sum_{\omega=0}^{\infty} j_{\omega} \cos \phi_{\omega} [\sin(\omega t - \phi_{\omega}) + \sin \phi_{\omega} e^{-\frac{t}{\tau}}]. \quad (\text{B.12})$$

Now the observed flow is

$$\frac{dV}{dt} = L_{PN} A_1 p + \frac{V_1}{\varepsilon} \frac{dp}{dt} \quad (\text{B.13})$$

where L_{PN} is the endosmotic hydraulic permeability of the cell.

Hence

$$\begin{aligned} \frac{dV}{dt} = & L_{PN} A_1 \frac{\tau \varepsilon A_2}{V_o} \sum_0^{\infty} j_{\omega} \cos \phi_{\omega} [\sin(\omega t - \phi_{\omega}) + \sin \phi_{\omega} e^{-\frac{t}{\tau}}] \\ & + \frac{V_1 \varepsilon \tau A_2}{\varepsilon V_o} \sum_0^{\infty} j_{\omega} \omega \cos \phi_{\omega} \left[\cos(\omega t - \phi_{\omega}) - \frac{1}{\omega \tau} \sin \phi_{\omega} e^{-\frac{t}{\tau}} \right]. \end{aligned} \quad (\text{B.14})$$

Now

$$L_{PN} = \frac{\beta A_2}{A_1 + A_2} L_p \quad (\text{B.15})$$

from the definition of β [Eq. (20)] and Eq. (17) in the text.

From Eqs. (B.15) and (B.4),

$$L_{PN} \frac{A_1 \tau \varepsilon A_2}{V_o} = \frac{A_1 A_2}{A_1 + A_2} \quad (\text{B.16})$$

and

$$\frac{V_1 A_2 \omega \tau \cos \phi_{\omega}}{V_o} = \frac{A_1 A_2 \sin \phi_{\omega}}{(A_1 + A_2 + \delta A)} \simeq \left(1 - \frac{\delta A}{A_1 + A_2} \right) \frac{A_1 A_2 \sin \phi_{\omega}}{(A_1 + A_2)} \quad (\text{B.17})$$

where it is assumed that the cell is a right cylinder so that $A \ll V$, and where δA represents the area of the cell in the stopper. Hence Eq. (B.14) becomes

$$\begin{aligned} \frac{dV}{dt} = & \frac{A_1 A_2}{A_1 + A_2} \sum_{\omega} j_{\omega} [\cos \phi_{\omega} \sin(\omega t - \phi_{\omega}) + \sin \phi_{\omega} \cos(\omega t - \phi_{\omega})] \\ & - \left(\frac{\delta A}{A_1 + A_2} \right) \left(\frac{A_1 A_2}{A_1 + A_2} \right) \sum_{\omega} j_{\omega} \sin \phi_{\omega} [\cos(\omega t - \phi_{\omega}) - \cos \phi_{\omega} e^{-\frac{t}{\tau}}] \end{aligned} \quad (\text{B.18})$$

$$\therefore \frac{dV}{dt} = \frac{A_1 A_2}{A_1 + A_2} \left(j - \frac{\delta A}{A_1 + A_2} \sum_{\omega} j_{\omega} \sin \phi_{\omega} [\cos(\omega t - \phi_{\omega}) - \cos \phi_{\omega} e^{-\frac{t}{\tau}}] \right) \quad (\text{B.19})$$

since

$$j = \sum_{\omega} j_{\omega} \sin \omega t$$

and in the limit as

$$\begin{aligned} \frac{\delta A}{A_1 + A_2} & \rightarrow 0 \\ \frac{dV}{dt} = & \frac{A_1 A_2 j}{A_1 + A_2}. \end{aligned} \quad (\text{B.20})$$

Appendix C

The Solution of the Equation Relating Subsequent Change in Turgor Pressure Owing to a Volume Flow in a Plant Cell Where the Recording Circuit Has a Finite Time Constant $\tau_2 = RC$

To solve Eq. (44) of the text,

$$\frac{dp'}{dt} + \frac{p'}{\tau_2} = \frac{\varepsilon A}{V_o} \frac{\tau}{\tau_2} \sum_{\omega=0}^{\infty} j_{\omega} \cos \phi_{\omega} [\sin(\omega t - \phi_{\omega}) + \sin \phi_{\omega} e^{-\frac{t}{\tau}}] \quad (\text{C.1})$$

where $p' = 0$ when $t = 0$,

$$\tau = \frac{V_o}{\epsilon \beta L_p A} \tag{C.2}$$

and also

$$\tau_2 = RC, \tag{C.3}$$

τ_2 being the time constant of the recording circuit.

As already mentioned, the solution of the homogeneous part of Eq. (C.1) is

$$p' = C_3 e^{\frac{-t}{\tau_2}} \tag{C.4}$$

from Eq. (43) where C_3 is an arbitrary constant to be determined from the initial conditions.

Rewriting Eq. (C.1) in exponentials

$$\frac{d p'}{d t} + \frac{p'}{\tau_2} = \frac{1}{\tau_2} \sum_{\omega=0}^{\infty} (B_{\omega} e^{i(\omega t - \phi_{\omega})} + i D_{\omega} e^{\frac{-t}{\tau}}) \tag{C.5}$$

where

$$B_{\omega} = \frac{\epsilon A \tau j_{\omega} \cos \phi_{\omega}}{V_o} = \frac{j_{\omega}}{\beta L_p} \cos \phi_{\omega}, \tag{C.6}$$

$$D_{\omega} = B_{\omega} \sin \phi_{\omega}, \tag{C.7}$$

and

$$i = \sqrt{-1}$$

and where only the imaginary part of the particular solution will be required. Try a trial solution:

$$p' = \sum_{\omega} (F_{\omega} e^{i(\omega t - \phi_{\omega})} + G_{\omega} e^{\frac{-t}{\tau}}) \tag{C.8}$$

where F_{ω} and G_{ω} are constants to be determined.

Substituting (C.8) into (C.5),

$$\begin{aligned} \sum_{\omega} \left(i \omega F_{\omega} e^{i(\omega t - \phi_{\omega})} - \frac{G_{\omega} e^{\frac{-t}{\tau}}}{\tau} \right) + \frac{1}{\tau_2} \sum_{\omega} (F_{\omega} e^{i(\omega t - \phi_{\omega})} + G_{\omega} e^{\frac{-t}{\tau}}) \\ = \frac{1}{\tau_2} \sum_{\omega} (B_{\omega} e^{i(\omega t - \phi_{\omega})} + i D_{\omega} e^{\frac{-t}{\tau}}). \end{aligned}$$

Since this must be identically true for all t , the coefficients of $e^{i(\omega t - \phi_{\omega})}$ and $e^{\frac{-t}{\tau}}$ may be equated so that,

$$F_{\omega} = \frac{B_{\omega}}{1 + i \omega \tau_2} \quad \text{and} \quad G_{\omega} = \frac{i \tau B_{\omega} \sin \phi_{\omega}}{(\tau - \tau_2)}.$$

Hence

$$\begin{aligned} p' = \sum_{\omega} B_{\omega} \left\{ \frac{(1 - i \omega \tau_2) e^{i(\omega t - \phi_{\omega})}}{(1 + (\omega \tau_2)^2)} + \frac{i \tau B_{\omega} \sin \phi_{\omega} e^{\frac{-t}{\tau}}}{(\tau - \tau_2)} \right\} \\ = \sum_{\omega} B_{\omega} \left\{ \frac{(1 - i \omega \tau_2) [\cos(\omega t - \phi_{\omega}) + i \sin(\omega t - \phi_{\omega})]}{(1 + (\omega \tau_2)^2)} + \frac{i \tau B_{\omega} \sin \phi_{\omega} e^{\frac{-t}{\tau}}}{(\tau - \tau_2)} \right\}. \end{aligned}$$

Taking only the imaginary part out,

$$p' = \sum_{\omega} B_{\omega} \left\{ \cos \theta_{\omega} [\cos \theta_{\omega} \sin(\omega t - \phi_{\omega}) - \sin \theta_{\omega} \cos(\omega t - \phi_{\omega})] + \frac{\tau \sin \phi_{\omega} e^{-\frac{t}{\tau}}}{(\tau - \tau_2)} \right\};$$

i.e.,

$$p' = \sum_{\omega} B_{\omega} \left\{ \cos \theta_{\omega} \sin(\omega t - \theta_{\omega} - \phi_{\omega}) + \frac{\tau \sin \phi_{\omega} e^{-\frac{t}{\tau}}}{\tau - \tau_2} \right\}$$

where

$$\theta_{\omega} = \tan^{-1} \omega \tau_2. \quad (\text{C.10})$$

Therefore the full solution from Eqs. (C.4) and (C.9) is

$$p' = C_3 e^{-\frac{t}{\tau_2}} + \sum_{\omega} B_{\omega} \left\{ \cos \theta_{\omega} \sin(\omega t - \theta_{\omega} - \phi_{\omega}) + \frac{\tau \sin \phi_{\omega} e^{-\frac{t}{\tau}}}{\tau - \tau_2} \right\}. \quad (\text{C.11})$$

However $p' = 0$ when $t = 0$; hence,

$$C_3 = \sum_{\omega} B_{\omega} \left\{ \cos \theta_{\omega} \sin(\theta_{\omega} + \phi_{\omega}) - \frac{\tau \sin \phi_{\omega}}{\tau - \tau_2} \right\}, \quad (\text{C.12})$$

and the solution becomes

$$p' = \sum_{\omega} B_{\omega} \left\{ \cos \theta_{\omega} [\sin(\omega t - \theta_{\omega} - \phi_{\omega}) + \sin(\theta_{\omega} + \phi_{\omega}) e^{-\frac{t}{\tau_2}}] + \frac{\tau \sin \phi_{\omega}}{\tau - \tau_2} [e^{-\frac{t}{\tau}} - e^{-\frac{t}{\tau_2}}] \right\}. \quad (\text{C.13})$$

Differentiating Eq. (C.13) with respect to time,

$$\frac{dp'}{dt} = \sum_{\omega} B_{\omega} \left\{ \cos \theta_{\omega} \left[\omega \cos(\omega t - \theta_{\omega} - \phi_{\omega}) - \frac{\sin(\theta_{\omega} + \phi_{\omega}) e^{-\frac{t}{\tau_2}}}{\tau_2} \right] - \frac{\tau \sin \phi_{\omega}}{\tau_2 - \tau} \left[-\frac{e^{-\frac{t}{\tau}}}{\tau} + \frac{e^{-\frac{t}{\tau_2}}}{\tau_2} \right] \right\}.$$

Substituting for B_{ω} from Eq. (C.6),

$$\frac{dp'}{dt} = \sum \frac{j_{\omega}}{\beta L_p} \left\{ \omega \cos \theta_{\omega} \cos \phi_{\omega} \cos(\omega t - \theta_{\omega} - \phi_{\omega}) - \frac{\cos \theta_{\omega} \cos \phi_{\omega} \sin(\theta_{\omega} + \phi_{\omega}) e^{-\frac{t}{\tau_2}}}{\tau_2} - \cos \phi_{\omega} \left(\frac{\tau \sin \phi_{\omega}}{\tau_2 - \tau} \right) \left[\frac{e^{-\frac{t}{\tau_2}}}{\tau_2} - \frac{e^{-\frac{t}{\tau}}}{\tau} \right] \right\}. \quad (\text{C.14})$$

Now both

$$\omega \tau \cos \phi_{\omega} = \sin \phi_{\omega} \quad (\text{C.15})$$

and

$$\omega \tau_2 \cos \theta_{\omega} = \sin \theta_{\omega} \quad (\text{C.16})$$

by the definitions of both ϕ_{ω} and θ_{ω} .

Hence

$$\begin{aligned} \frac{dp'}{dt} &= \sum \frac{j_\omega}{\beta L_p} \sin \phi_\omega \left\{ \frac{\cos \theta_\omega}{\tau} \cos(\omega t - \theta_\omega - \phi_\omega) \right. \\ &\quad \left. - \frac{\cos \theta_\omega \cos \phi_\omega \sin(\theta_\omega + \phi_\omega) e^{-\frac{t}{\tau_2}}}{\tau_2 \sin \phi_\omega} \right. \\ &\quad \left. - \frac{\tau \cos \phi_\omega}{\tau_2 - \tau} \left[\frac{e^{-\frac{t}{\tau_2}}}{\tau_2} - \frac{e^{-\frac{t}{\tau}}}{\tau} \right] \right\}; \\ \therefore \frac{dp'}{dt} &= \frac{1}{\beta L_p} \sum j_\omega \sin \phi_\omega \left[\frac{\cos \theta_\omega}{\tau} \cos(\omega t - \theta_\omega - \phi_\omega) + \frac{\cos \phi_\omega e^{-\frac{t}{\tau}}}{\tau_2 - \tau} \right. \\ &\quad \left. - \frac{\cos \theta_\omega \cos \phi_\omega \sin(\theta_\omega + \phi_\omega) e^{-\frac{t}{\tau_2}}}{\tau_2 \sin \phi_\omega} - \frac{\tau \cos \phi_\omega e^{-\frac{t}{\tau_2}}}{\tau_2(\tau_2 - \tau)} \right]; \\ \therefore \frac{dp'}{dt} &= \frac{1}{\beta L_p} \sum j_\omega \sin \phi_\omega \left[\frac{\cos \theta_\omega}{\tau} \cos(\omega t - \theta_\omega - \phi_\omega) + \frac{\cos \phi_\omega e^{-\frac{t}{\tau}}}{\tau_2 - \tau} \right. \\ &\quad \left. - \frac{\cos \theta_\omega (\sin \theta_\omega \cos \phi_\omega + \cos \theta_\omega \sin \phi_\omega) e^{-\frac{t}{\tau_2}}}{\omega \tau_2 \tau} - \frac{\tau \cos \phi_\omega e^{-\frac{t}{\tau_2}}}{\tau_2(\tau_2 - \tau)} \right]. \quad (C.17) \end{aligned}$$

Using Eq. (C.15) and expanding, Eq. (C.17) becomes:

$$\begin{aligned} \frac{dp'}{dt} &= \frac{1}{\beta L_p} \sum j_\omega \sin \phi_\omega \left[\frac{\cos \theta_\omega}{\tau} \cos(\omega t - \theta_\omega - \phi_\omega) + \frac{\cos \phi_\omega e^{-\frac{t}{\tau}}}{\tau_2 - \tau} \right. \\ &\quad \left. - \frac{\cos \theta_\omega}{\tau} (\cos \theta_\omega \cos \phi_\omega - \sin \theta_\omega \sin \phi_\omega) e^{-\frac{t}{\tau_2}} - \frac{\sin \phi_\omega e^{-\frac{t}{\tau_2}}}{\omega \tau_2 \tau} - \frac{\tau \cos \phi_\omega e^{-\frac{t}{\tau_2}}}{\tau_2(\tau_2 - \tau)} \right] \end{aligned}$$

using the identity $\cos^2 A \equiv 1 - \sin^2 A$.

Therefore,

$$\begin{aligned} \frac{dp'}{dt} &= \frac{1}{\beta L_p} \sum j_\omega \sin \phi_\omega \left[\frac{\cos \theta_\omega}{\tau} \{ \cos(\omega t - \theta_\omega - \phi_\omega) - \cos(\theta_\omega + \phi_\omega) e^{-\frac{t}{\tau_2}} \} \right. \\ &\quad \left. + \frac{\cos \phi_\omega}{(\tau_2 - \tau)} \{ e^{-\frac{t}{\tau}} - e^{-\frac{t}{\tau_2}} \} \right]. \quad (C.18) \end{aligned}$$

Appendix D

A Calculation of the Volume Flow Caused by Local Concentration Enhancement in the Cell Wall During an Action Potential

The differential equation considered in this appendix is somewhat similar to many of those considered by Carslaw and Jaeger (1959) in their excellent treatise on heat

conduction, and the solution follows closely their application of the Laplace transform method (see also Barry & Hope, 1969*a*). The equation is the same as Eq. (49) of the text.

$$\frac{\partial^2 c}{\partial r^2} + \frac{1}{r} \frac{\partial c}{\partial r} = \frac{1}{D} \frac{\partial c}{\partial t} \quad (\text{D.1})$$

with the boundary condition

$$D \left(\frac{\partial c}{\partial r} \right)_a = j_\omega \sin \omega t. \quad (\text{D.2})$$

Taking the Laplace transform of both equations results in

$$\frac{d^2 \bar{c}}{dr^2} + \frac{1}{r} \frac{d\bar{c}}{dr} = p \frac{\bar{c}}{D} \quad (\text{D.3})$$

and

$$D \left(\frac{d\bar{c}}{dr} \right)_a = j_\omega \frac{\omega}{p^2 + \omega^2} \quad (\text{D.4})$$

where $\bar{c}(r) = \int_0^\infty e^{-pt} c(r, t) dt$, where p is such that its real part is sufficiently large so that the integral converges. There is also the condition that \bar{c} is finite as $r \rightarrow 0$.

The solution satisfying Eq. (D.3) and the above boundary condition is

$$\bar{c} = AI_0(qr) \quad (\text{D.5})$$

where

$$q^2 = \frac{p}{D}; \quad (\text{D.6})$$

A is an arbitrary constant and I_0 is a hyperbolic Bessel function of order "0".

Hence at $r = a$,

$$D \left(\frac{d\bar{c}}{dr} \right)_a = DAqI_1(qa) = j_\omega \frac{\omega}{p^2 + \omega^2} \quad (\text{D.7})$$

so that

$$\bar{c} = \frac{j_\omega \omega}{Dq(p^2 + \omega^2)} \cdot \frac{I_0(qr)}{I_1(qa)} \quad (\text{D.8})$$

and I_1 is a hyperbolic Bessel function of order "1".

The solution of this equation is given by the inversion transform (Carslaw & Jaeger, 1961), namely

$$c = \frac{j_\omega/D}{2\pi i} \int_{\gamma-i\infty}^{\gamma+i\infty} \frac{\omega I_0(\mu r) e^{\lambda t}}{\mu(\lambda^2 + \omega^2) I_1(\mu a)} d\lambda \quad (\text{D.9})$$

where the contour is as in Fig. 13 of Barry & Hope (1969*a*), and μ and λ are again written for q and p .

Evaluation of this integral proceeds by using Cauchy's formula, and the solution merely involves calculating the residues at the various poles (Phillips, 1957; Jaeger, 1961) and multiplying by $2\pi i$.

(i) At $\lambda = \pm i\omega$ and $\mu = \pm \left(\pm i \frac{\omega}{D} \right)^{\frac{1}{2}}$,

The residues of the integrand of Eq. (D.9) for both poles are

$$\frac{I_0 \left[r \left(\frac{\omega}{D} i \right)^{\frac{1}{2}} \right] e^{i\omega t}}{2i \left(i \frac{\omega}{D} \right)^{\frac{1}{2}} \cdot I_1 \left[a \left(i \frac{\omega}{D} \right)^{\frac{1}{2}} \right]} - \frac{I_0 \left[r \left(-i \frac{\omega}{D} \right)^{\frac{1}{2}} \right] e^{-i\omega t}}{2i \left(-i \frac{\omega}{D} \right)^{\frac{1}{2}} \cdot I_1 \left[a \left(-i \frac{\omega}{D} \right)^{\frac{1}{2}} \right]}.$$

(ii) At $\lambda=0$, the integrand of Eq. (D.9) may be expanded for λ small so that it becomes approximately

$$\frac{2D(1 + \lambda t + \dots) \left(1 + \frac{r^2 \lambda}{4D} + \dots \right) \left(1 - \frac{\lambda a^2}{8D} + \dots \right) \left(1 - \frac{\lambda^2}{\omega^2} + \dots \right)}{\omega a \lambda}.$$

The coefficient of λ^{-1} is then $\frac{2D}{\omega a}$ and the residue is thus $\frac{2j_\omega}{\omega a}$. At $\lambda = -D\alpha_m'^2$, by the residue formula (McLachlan, 1953, p. 54) the residue is

$$2 \sum_m \frac{j_\omega \omega e^{-D\alpha_m'^2 t} J_0(\alpha_m' r)}{a(D^2 \alpha_m'^4 + \omega^2) J_0(\alpha_m' a)}$$

where α_m is a zero of $J_1(\alpha_m)$ and $\alpha_m = a\alpha_m'$.

Thus the full solution at $r=a$ becomes

$$c(a) = \frac{2j_\omega}{\omega a} + \frac{j_\omega}{D} \left\{ \frac{I_0 \left[a \left(i \frac{\omega}{D} \right)^{\frac{1}{2}} \right] e^{i\omega t}}{2i \left(i \frac{\omega}{D} \right)^{\frac{1}{2}} \cdot I_1 \left[a \left(i \frac{\omega}{D} \right)^{\frac{1}{2}} \right]} - \frac{I_0 \left[a \left(-i \frac{\omega}{D} \right)^{\frac{1}{2}} \right] e^{-i\omega t}}{2i \left(-i \frac{\omega}{D} \right)^{\frac{1}{2}} \cdot I_1 \left[a \left(-i \frac{\omega}{D} \right)^{\frac{1}{2}} \right]} \right\} + 2 \sum_m \frac{j_\omega \omega e^{-D\alpha_m'^2 t}}{a(D^2 \alpha_m'^4 + \omega^2)}. \tag{D.10}$$

Now $(\pm i)^{\frac{1}{2}} = i^{\pm \frac{1}{2}}$ and since the following relationships hold (see McLachlan, 1955, pp. 137-141)

$$I_0 [z(i)^{\pm \frac{1}{2}}] = M_0(z) e^{\pm i\theta_0(z)}$$

and

$$i^{\pm \frac{1}{2}} I_1 [z(i)^{\pm \frac{1}{2}}] = M_1(z) e^{\pm i(\theta_1(z) - \frac{\pi}{4})},$$

then

$$\frac{I_0(z i^{\frac{1}{2}}) e^{i\omega t}}{i^{\frac{1}{2}} I(z i^{\frac{1}{2}})} = \frac{M_0(z) e^{i[\theta_0(z) - \theta_1(z) + \frac{\pi}{4} + \omega t]}}{M_1(z)} \tag{D.11}$$

where M_0 and M_1 are moduli of the kindred Bessel functions of order 0 and 1, and θ_0 and θ_1 are the corresponding arguments as defined in McLachlan (1955). Similarly

$$\frac{I_0(z i^{-\frac{1}{2}}) e^{-i\omega t}}{i^{-\frac{1}{2}} \cdot I_1(z i^{-\frac{1}{2}})} = \frac{M_0(z) e^{-i[\theta_0(z) - \theta_1(z) + \frac{\pi}{4} + \omega t]}}{M_1(z)}. \tag{D.12}$$

Adding Eqs. (D.11) and (D.12) and substituting back into Eq. (D.10), the solution becomes

$$c(a) = 2j_\omega \left\{ \frac{1}{\omega a} + \frac{M_0[a\sqrt{\omega/D}]}{2\sqrt{\omega D} \cdot M_1[a\sqrt{\omega/D}]} \right. \\ \cdot \sin \left[\omega t + \theta_0(a\sqrt{\omega/D}) - \theta_1(a\sqrt{\omega/D}) + \frac{\pi}{4} \right] \\ \left. + \frac{\omega}{a} \sum_{m=1}^{\infty} \frac{e^{-D\alpha_m^2 t/a^2}}{(D^2 \alpha_m^4/a^4 + \omega^2)} \right\} \quad (\text{D.13})$$

where α_m is a zero of $J_1(\alpha_m)$.

Hence the volume flow is given for a uni-univalent electrolyte as

$$J_v = 2\sigma L_p RTc(a) \quad (\text{D.14})$$

with the value of $c(a)$ obtained from Eq. (D.13).

References

- Allen, R. D. 1969. Mechanism of the seismonastic reaction in *Mimosa pudica*. *Plant Physiol.* **44**:1101.
- Barry, P. H. 1967. Investigation of the movement of water and ions in plant cell membranes. Ph. D. Thesis. University of Sydney, Sydney, Australia.
- 1970. Volume flows and pressure changes during an action potential in cells of *Chara Australis*. I. Experimental results. *J. Membrane Biol.* **3**:313.
- Hope, A. B. 1969a. Electro-osmosis in membranes: Effects of unstirred layers and transport numbers. Part I. Theory. *Biophys. J.* **9**:700.
- — 1969b. Electro-osmosis in membranes: Effects of unstirred layers and transport numbers. Part II. Experimental. *Biophys. J.* **9**:729.
- — 1969c. Electro-osmosis in *Chara* and *Nitella* cells. *Biochim. Biophys. Acta* **193**:124.
- Carslaw, H. S., Jaeger, J. C. 1959. Conduction of Heat in Solids. The Clarendon Press, Oxford.
- Comrie, L. J. 1955. Chamber's Shorter Six-Figure Mathematical Tables. W. & R. Chambers Ltd., London.
- Courant, R. 1937. Differential and Integral Calculus, Vol. I. Blackie and Sons, Ltd., London and Glasgow.
- Dainty, J., Ginzburg, B. Z. 1964. The measurement of hydraulic conductivity (osmotic permeability to water) of internodal *Characean* cells by means of transcellular osmosis. *Biochim. Biophys. Acta* **79**:102–111.
- Fensom, D. S. 1966. Action potentials and associated waterflows in living *Nitella*. *Canad. J. Botany* **44**:1432.
- Gaffey, C. T., Mullins, L. J. 1958. Ion fluxes during the action potential in *Chara*. *J. Physiol.* **144**:505.
- Hope, A. B., Findlay, G. P. 1964. The action potential in *Chara*. *Plant Cell. Physiol.* **5**:377.
- Jaeger, J. C. 1961. An Introduction to the Laplace Transformation. Methuen and Co. Ltd., London.
- Kamiya, N., Tazawa, M. 1956. Studies on the water permeability of a single plant cell by means of transcellular osmosis. *Protoplasma* **46**:394.
- — Takata, T. 1963. The relation of turgor pressure to cell volume in *Nitella* with special reference to the mechanical properties of the cell wall. *Protoplasma* **57**:501.

- Katchalsky, A., Kedem, O. 1962. Thermodynamics of flow processes in Biological systems. *Biophys. J.* **2**:53.
- Kedem, O., Katchalsky, A. 1958. Thermodynamic analysis of the permeability of biological membranes to non-electrolytes. *Biochim. Biophys. Acta* **27**:229.
- Kelly, R. B., Kohn, P. G., Dainty, J. 1963. Water relations of *Nitella translucens*. *Trans. Botan. Soc.* **39**:373.
- Kishimoto, U., Ohkawa, T. 1966. Shortening of *Nitella* internode during excitation. *Plant Cell Physiol.* **7**:493.
- Kobatake, Y., Fujita, O. 1964*a*. Flows through charged membranes. I. Flip-flop current vs. voltage relation. *J. Chem. Phys.* **40**:2212.
- — 1964*b*. Flows through charged membranes. II. Oscillation phenomena. *J. Chem. Phys.* **40**:2219.
- McLachlan, N. W. 1953. Complex Variable Theory and Transform Calculus. Cambridge University Press, Cambridge.
- 1955. Bessel Functions for Engineers. The Clarendon Press, Oxford.
- Mailman, D. S., Mullins, L. J. 1966. The electrical measurement of chloride fluxes in *Nitella*. *Aust. J. Biol. Sci.* **19**:385.
- Phillips, E. G. 1957. Functions of a Complex Variable. Oliver and Boyd, Edinburgh and London.
- Tazawa, M., Kamiya, N. 1965. Water relations of *Characean* internodal cell. *Ann. Report of Biol. Works. Faculty of Science, Osaka University* **13**:123.
- — 1966. Water permeability of *Characean* internodal cell with special reference to its polarity. *Aust. J. Biol. Sci.* **19**:399.
- Teorell, T. 1958. Transport processes in membranes in relation to the nerve mechanism. *Exp. Cell Res.* **5**:83.
- 1959*a*. Electrokinetic membrane processes in relation to properties of excitable tissues. I. Experiments on oscillatory transport phenomena in artificial membranes. *J. Gen. Physiol.* **42**:831.
- 1959*b*. Electrokinetic membrane processes in relation to properties of excitable tissues. II. Some theoretical considerations. *J. Gen. Physiol.* **42**:847.
- 1961. An analysis of the current-voltage relationships in excitable *Nitella* cells. *Acta Physiol. Scand.* **53**:1.
- 1962. Excitability phenomena in artificial membranes. *Biophys. J.* **2**:27.
- 1966. Electrokinetic considerations of mechanoelectric transduction. *Ann. N.Y. Acad. Sci.* **137**:950.
- Watson, G. N. 1944. Theory of Bessel Functions. Cambridge University Press, Cambridge, England.
- Wirth, H. E. 1937. The partial molal volumes of potassium chloride, potassium bromide and potassium sulfate in sodium chloride solutions. *J. Amer. Chem. Soc.* **59**:2549.